Electron. Mater. Lett., Vol. 9, No. 6 (2013), pp. 851-854
DOI: 10.1007/s13391-013-6028-0

Improved Electrochemical Performance of Doped-$LiNi_{0.5}Mn_{1.5}O_4$ Cathode Material for Lithium-Ion Batteries

Hyun-Ju Kim,[1] Bong-Soo Jin,[1] Chil-Hoon Doh,[1] Dong-Sik Bae,[2] and Hyun-Soo Kim[1,*]

[1]Battery Research Center, Korea Electrotechnology Research Institute, Changwon 641-120, Korea
[2]Changwon National University, Changwon 641-773, Korea

(received date: 19 September 2012 / accepted date: 9 January 2013 / published date: 10 November 2013)

In this paper, the electrochemical performance of doped-$LiNi_{0.5}Mn_{1.5}O_4$ is reviewed. The rate capability, rate performance, and cyclic life of the doped-$LiNi_{0.5}Mn_{1.5}O_4$ materials with various elements are reported. The Fe, Sc-substituted materials exhibited remarkably superior cycling performance and rate capabilities than pristine $LiNi_{0.5}Mn_{1.5}O_4$.

Keywords: lithium-ion battery, doped-$LiNi_{0.5}Mn_{1.5}O_4$, cathode active material, solid-state reaction method, polyvinyl butyral (PVB)

1. INTRODUCTION

Spinel $LiMn_2O_4$ has been investigated widely because Mn is inexpensive and environmentally benign. However, $LiMn_2O_4$ exhibits severe capacity fade on cycling, particularly at elevated temperatures. With an aim to overcome these capacity fading problems, several cationic substitutions to give $LiM_xMn_{2-x}O_4$ (M = Cr, Fe, Co, Ni, and Cu) have been pursued.[1-4] The capacity and voltage plateau in Li/$LiM_xMn_{2-x}O_4$ cells strongly depend on the kinds of transition metals and their contents. Among those materials, $LiNi_{0.5}Mn_{1.5}O_4$ has received great attention due to its dominant potential plateau at around 4.7 V. Moreover, $LiNi_{0.5}Mn_{1.5}O_4$ has shown the highest discharge capacity with stable cycleability in this high potential range.

In recent years, many methods to synthesize $LiNi_{0.5}Mn_{1.5}O_4$ have been reported, including the solid-state method, sol-gel method, co-precipitation method, composite carbonate process, molten salt method, emulsion drying method, and ultrasonic spray pyrolysis method.[5-8] Different synthesizing methods may result in products with different properties.[9] During the synthesis of $LiNi_{0.5}Mn_{1.5}O_4$, secondary phases, such as NiO and $Li_xNi_{1-x}O$, usually exist in the products due to the oxygen loss at high temperature, and this can degrade the electrochemical behavior.[10]

Fortunately, cationic substitutions help to eliminate the formation of the $Li_xNi_{1-x}O$ impurity phase and stabilize the spinel structure with a disordering of the Mn^{4+} and Ni^{2+} ions in the 16d octahedral sites instead of the cation-ordered structure formed by the pristine $LiNi_{0.5}Mn_{1.5}O_4$. These results in a smaller lattice parameter difference among the three cubic phases formed during cycling and improved electrochemical performance.

Therefore, we focus here on various cationic substitutions in $LiNi_{0.5}Mn_{1.5}O_4$ via a modified-solid-state reaction method. Generally, carbonates or hydroxides have been used as starting materials for solid-state reaction methods.[11] However, a modified solid-state reaction method was adapted using an iron oxalate source instead of carbonate in this study. The organic functional group oxalate inhibits the growth of primary particles. Thus, we can expect that it would lead to an increased specific capacity due to the formation of small particles. Also, some residual carbon from the organic functional group should remain among the primary particles after calcination. This improves the electronic conductivity of secondary particles. Also, the crystal structure and morphology of the synthesized doped-$LiNi_{0.5}Mn_{1.5}O_4$ were analyzed and their electrochemical properties were also evaluated.

2. EXPERIMENTAL PROCEDURE

Carbon-coated $LiNi_{0.45}X_{0.05}Mn_{1.5}O_4$ (X = Mo, Fe, Mg, Sc) powder precursors were synthesized using stoichiometric amounts of Li_2CO_3, NiC_2O_4, $MnCO_3$, and transitional metal sources, which were thoroughly mixed using a ball mill. Also, polyvinyl butyral (PVB) was used as a carbon source to produce carbon in situ to improve the electrical conductivity of the $LiNi_{0.45}X_{0.05}Mn_{1.5}O_4$. Then, the sample was heat-treated by a two-step calcination process. In the first step (450°C for 5 h), destruction of the carbonate metal precursors took place, yielding semicrystallized powders. In the subsequent step, a high-temperature treatment (850°C for

*Corresponding author: hskim@keri.re.kr

10 h) was applied to achieve well-crystallized spinel $LiNi_{0.5}Mn_{1.5}O_4$ powders.

X-ray diffraction analysis was performed to observe the crystal structure and any impurities in the synthesized active material, using an X-pert PW3830 (Philips Co.). The Cu Kα line was used under conditions of 40 kV and 30 mA, with a scan speed of 0.04°/sec. In addition, field emission SEM (S-4800, Hitachi Co.) analysis was conducted to measure the particle size and observe the surface morphology.

The active material, a conducting agent (Super-P carbon black), and a binder (polyvinylidene fluoride), were dispersed in *N*-methylpyrrolidone at a ratio of 80 : 10 : 10 (wt. %) to obtain a slurry. The slurry was then coated onto aluminum foil and dried for 12 h at 100°C. Next, the material was pressed using a hot roll press at 110°C. The cathode electrode thus produced, a lithium anode, and a separator (Celgard 3501) were laminated for assembly into coin cells (CR2032 type). A 1 M solution of $LiPF_6$ in 1 : 1 ethylene carbonate / dimethyl carbonate (vol. %) was used as the electrolyte.

The electrochemical performance of the synthesized $LiNi_{0.5}Mn_{1.5}O_4$/C cathode materials was measured using a battery test system (TOSCAT-3100, Toyo System Co.). The materials were charged and discharged over a voltage range of 3.0 - 4.9 V by the constant current–constant voltage method. Rate capability was evaluated at current rates of 0.1 - 20 C. The cycling performance of the synthesized material was also tested at a current rate of 0.3 C. EIS was conducted for the discharged cell using an IM6 electrochemical workstation (ZAHNER-Elektrik). The frequency was measured in the range of 1 Hz - 1 MHz, and the amplitude was measured at 10 mV.

3. RESULTS AND DISCUSSION

The XRD patterns of the pristine and doped-$LiNi_{0.5}Mn_{1.5}O_4$ samples are shown in Fig. 1. All samples were identified and indexed to the cubic spinel structure with typical intensive peaks, such as (111), (311), (400), and (440). Moreover, there were no other peaks corresponding to undesired second phases, such as $Li_xNi_{1-x}O$, which usually appears in oxygen nonstoichiometric spinels.[12] Moreover, there were no obvious differences between the diffraction patterns of the $LiNi_{0.45}X_{0.05}Mn_{1.5}O_4$ synthesized under different conditions except for the $LiNi_{0.45}Mo_{0.05}Mn_{1.5}O_4$ samples. Note that the slight peaks representing Mn_3O_4 impurities appear on the left of the (111), (311), and (511) peaks in the XRD pattern, as shown in Fig. 1.

Figure 2 shows the FE-SEM images of the cation-substituted samples. The particle size of the cation-substituted samples was about 1 - 3 μm. Also, all samples exhibited an octahedral morphology with smooth (111) facets. It has been reported that $LiNi_{0.5}Mn_{1.5}O_4$ with clear (111) facets has excellent electrochemical behavior because Li-ion transportation into the electrolyte is fastest through (111) facets. In addition, $LiNi_{0.5}Mn_{1.5}O_4$/C with an octahedral shape possesses the lowest internal stress during the lithium ion deintercalation/intercalation process.[13]

The charge/discharge curves at the current rate of 0.1 C for

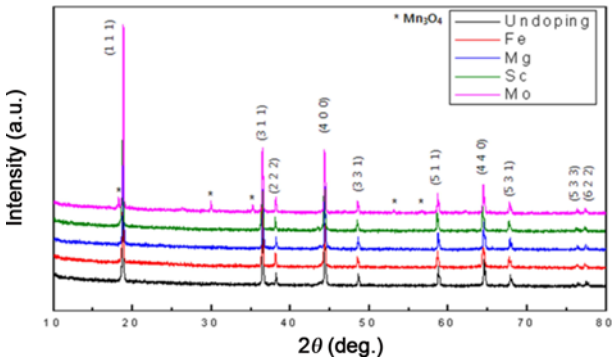

Fig. 1. XRD patterns of the pristine and doped-$LiNi_{0.5}Mn_{1.5}O_4$ samples.

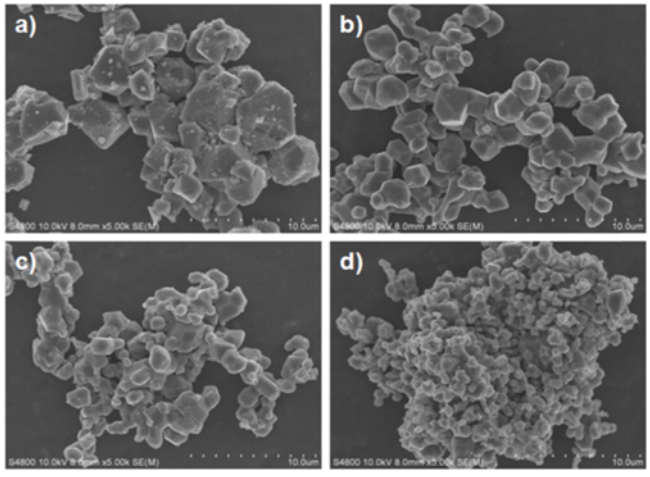

Fig. 2. FE-SEM images of the cation-substituted $LiNi_{0.45}X_{0.05}Mn_{1.5}O_4$ samples. (a) Mo, (b) Fe, (c) Sc, and (d) Mg.

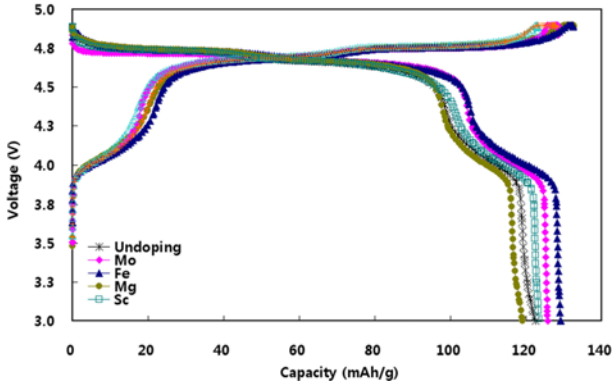

Fig. 3. Initial charge-discharge curves of the $LiNi_{0.5}Mn_{1.5}O_4$ and $LiNi_{0.45}X_{0.05}Mn_{1.5}O_4$ samples.

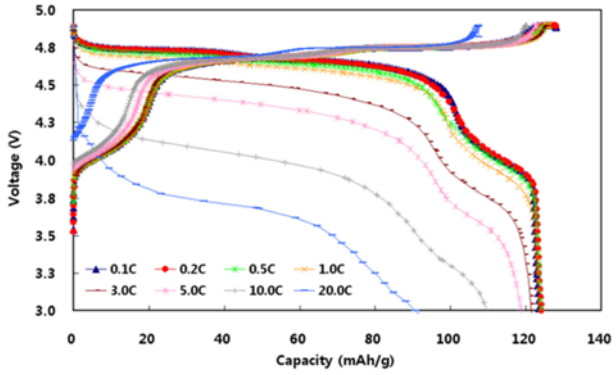

Fig. 4. Rate capability results of the $LiNi_{0.45}Sc_{0.05}Mn_{1.5}O_4$ sample.

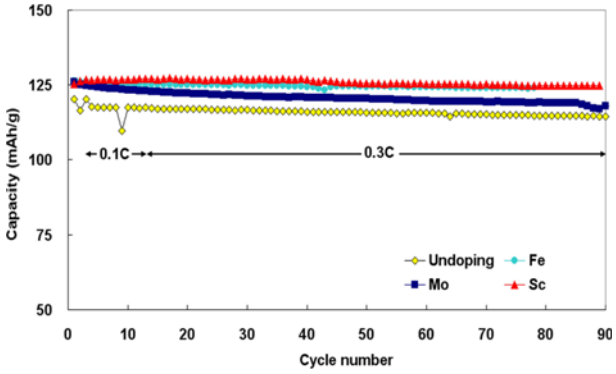

Fig. 5. Cycling performance of the $LiNi_{0.5}Mn_{1.5}O_4$ and $LiNi_{0.45}X_{0.05}Mn_{1.5}O_4$ samples.

$LiNi_{0.45}X_{0.05}Mn_{1.5}O_4$/C synthesized under different cation-substituted samples are shown in Fig. 3. The initial discharge capacities for the pristine and doped-$LiNi_{0.5}Mn_{1.5}O_4$ samples were 123 - 130 mAh g^{-1}. All of the samples display three plateaus, one at 4.1 and two at approximately 4.7 V. The plateau at 4.1 V is from the redox process of Mn^{3+}/Mn^{4+}, while the two plateaus at 4.7 V are caused by the Ni^{2+}/Ni^{3+} and Ni^{3+}/Ni^{4+} transitions.[13]

Figure 4 shows the rate capability of the $LiNi_{0.45}Sc_{0.05}Mn_{1.5}O_4$ samples. The discharge capacities of the $LiNi_{0.45}Sc_{0.05}Mn_{1.5}O_4$/C composites were 123.5, 124.2, 124, 123.7, 121.4, and 118.7 $mAhg^{-1}$ at the 0.1, 0.2, 0.5, 1.0, 2.0, and 5.0 C rate, respectively. Also, the excellent discharging capacity of 110.1 $mAhg^{-1}$ was observed at the high discharge current rate (10.0 C).

The cycling behaviors of the $LiNi_{0.5}Mn_{1.5}O_4$ and $LiNi_{0.45}X_{0.05}Mn_{1.5}O_4$ composites are shown in Fig. 5. Cycling began with five charging/ discharging formations at 0.1 C executed 90 times. All the samples showed excellent cycling behaviors at the rate of 0.3 C. This can be attributed to the enhancement of electrical conductivity caused by the carbon coating and to the excellent cycle ability of $LiNi_{0.5}Mn_{1.5}O_4$/C itself due to the high stability of the spinel structure and the minor

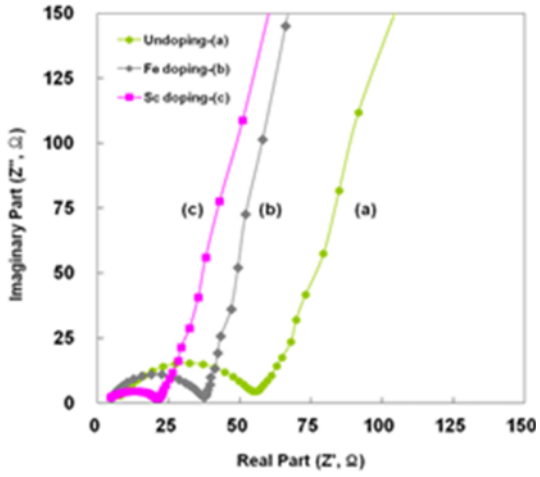

Fig. 6. Nyquist plots of the $LiNi_{0.5}Mn_{1.5}O_4$ and $LiNi_{0.45}X_{0.05}Mn_{1.5}O_4$ samples.

lattice adjustment upon cycling. Notably, $LiNi_{0.45}Sc_{0.05}Mn_{1.5}O_4$ samples exhibited identically good discharge capacity ~124.7 mAh g^{-1} with excellent capacity retentions over 98.4% after 90 cycles.

EIS was applied to further analyze the effect of cation-substitution, as shown in Fig. 6. The Nyquist plots of all the samples showed an intercept at high frequency, followed by a semicircle in the middle- and high-frequency region and a straight line in the low-frequency region.[14] In the middle-high frequency region, after cation-substituted $LiNi_{0.45}X_{0.05}Mn_{1.5}O_4$ (X = Fe, Sc), the sample exhibited a smaller charge-transfer resistance (below 35 Ω) than that of the pristine $LiNi_{0.5}Mn_{1.5}O_4$ (55 Ω). The charge-transfer resistance was the lowest at 21 Ω in the case of the $LiNi_{0.45}Sc_{0.05}Mn_{1.5}O_4$ sample. Thus, cationic substitutions help eliminate the formation of the $Li_xNi_{1-x}O$ impurity phase and stabilize the spinel structure with a disordering of the Mn^{4+} and Ni^{2+} ions in the 16d octahedral sites instead of the cation-ordered structure formed by the pristine $LiNi_{0.5}Mn_{1.5}O_4$. These results in a smaller lattice parameter difference among the three cubic phases formed during cycling and improved electrochemical performance.

4. CONCLUSIONS

The partial substitution of cations in spinel-structured $LiNi_{0.5}Mn_{1.5}O_4$ was synthesized via a modified solid-state reaction method. The substitution of Fe and Sc in $LiNi_{0.45}X_{0.05}Mn_{1.5}O_4$ has been found to significantly improve the cycling performance and rate capability. In particular, the $LiNi_{0.45}Sc_{0.05}Mn_{1.5}O_4$ sample with the substitution of Sc for Ni delivers a capacity of 124.7 mAh/g at the 0.3 C rate with the capacity retention of 98.4% after 90 charge/discharge cycles and a remarkably high capacity of 90 mAh/g at a C-rate of 20.

ACKNOWLEDGMENTS

This work was supported by the Korea Evaluation Institute of Industrial Technology (KEIT) grant funded by the Korean government Ministry of Knowledge Economy (No. 10039182).

REFERENCES

1. M. Obrovac and Y. Gao, J. Dahn, *Phys. Rev.* **B57**, 5728 (1998).
2. C. Sigala, D. Guyomard, A. Verbaere, Y. Diffard, and M. Tournoux, *Solid State Ionics* **81**, 167 (1995).
3. H. Kawai, M. Nagata, M. Tabuchi, H. Tukamoto, and A. West, *Chem. Mater.* **10**, 3266 (1998).
4. H. Fang, Z. Wang, X. Li, H. Guo, and W. Peng, *J. Power Sources* **153**, 174 (2006).
5. Y. Fan, J. Wang, X. Ye, and J. Zhangg, *J. Mater. Chem. Phys.* **103**, 19 (2007).
6. G. Liu, Y. Wang, L. Qi, W. Li, and H. Chen, *Electrochim. Acta* **50**, 1965 (2005).
7. J. Kim, S. Myung, and Y. Sun, *Electrochim. Acta* **49**, 219 (2004).
8. S. Park and Y. Sun, *Electrochim. Acta* **50**, 431 (2004).
9. J. Arrebola, A. Caballero, and M. Cruz, *J. Adv. Func. Mater.* **16**, 1904 (2006).
10. R. Alcantara, M. Jaraba, P. Lavela, and J. Tirada, *Electrochim. Acta* **47**, 1829 (2002).
11. Y. Lee, Y. Sun, S. Ota, T. Miyashita, and M. Yoshio, *Electrochem. Commun.* **4**, 989 (2002).
12. Y. Oh, S. Nam, S. Wi, S. Hong, and B. Park, *Electron. Mater. Lett*. **8**, 91 (2012).
13. H. Xia, S. Tang, L. Lu, Y. Meng, and G. Ceder, *Electrochim. Acta* **52**, 2822 (2007).
14. A. Yamada, S. Chung, and K. Hinokuma, *J. Electrochem. Soc*. **148**, A224 (2001).